

Increased vegetation growth and carbon stock in China karst via ecological engineering

Xiaowei Tong¹, Martin Brandt², Yuemin Yue^{1,3*}, Stephanie Horion², Kelin Wang^{1,3*}, Wanda De Keersmaecker⁴, Feng Tian², Guy Schurgers², Xiangming Xiao^{5,6}, Yiqi Luo^{5,7,8}, Chi Chen⁹, Ranga Myneni⁹, Zheng Shi⁵, Hongsong Chen^{1,3} and Rasmus Fensholt²

Afforestation and reforestation projects in the karst regions of southwest China aim to combat desertification and improve the ecological environment. However, it remains unclear at what scale conservation efforts have impacted on carbon stocks and if vegetation regrowth occurs at a large spatial scale as intended. Here we use satellite time series data and show a widespread increase in leaf area index (a proxy for green vegetation cover), and aboveground biomass carbon, which contrasted negative trends found in the absence of anthropogenic influence as simulated by an ecosystem model. In spite of drought conditions, aboveground biomass carbon increased by 9% (+0.05 Pg C y⁻¹), mainly in areas of high conservation effort. We conclude that large scale conservation projects can contribute to a greening Earth with positive effects on carbon sequestration to mitigate climate change. At the regional scale, such ecological engineering projects may reduce risks of desertification by increasing the vegetation cover and reducing the ecosystem sensitivity to climate perturbations.

The impacts of climate change and anthropogenic activities on Earth's vegetation and ecosystems have been in the spotlight of science in the past decades^{1–6}. With increasing climate variability and more frequent occurrences of extreme events expected in the future⁷, research has targeted the sensitivity of ecosystems^{8,9}. At the same time, recent studies have shown globally increasing leaf area index (LAI; a proxy for green vegetation cover)¹⁰, and aboveground biomass carbon (ABC)¹¹, also known as the greening Earth^{10,12}. Dynamic vegetation models and Earth observation studies reveal climatic and atmospheric changes as the main drivers of large scale increases in LAI^{10,13}. On the contrary, the anthropogenic footprint is usually found to cause land degradation and deforestation^{13,14}, and only a few studies find a direct positive effect of management on vegetation cover and biomass trends^{2,11,15}. Although ecological conservation projects aim at increasing biodiversity, carbon sequestration and vegetation cover^{16,17}, the success of such conservation efforts is not easily quantifiable, and the spatial footprint of projects is not always commensurable with contemporary satellite- and modelling-based monitoring methods. Adaptation and mitigation strategies to climate change should be anchored in knowledge on how ecosystems respond to climatic and anthropogenic disturbances, but at present it is not known whether conservation projects impact on the ability of vegetation to alleviate the effects of climate change at large scales.

China's ecological restoration projects (for example, the Natural Forest Protection Project, the Grain to Green Project, and the Karst Rocky Desertification Restoration Project) are considered 'mega-engineering' activities and the most ambitious afforestation and conservation projects in human history^{16–19}. The highly sensitive and

vulnerable karst ecosystem in southwest China is one of the largest exposed carbonate rock areas (more than 0.54 million km²) in the world. This area hosts 220 million people^{20,21} and has been selected as a major target of restoration projects. Descriptions as early as the seventeenth century reported the rocky karst mountains as an area of sparse forest or vegetation cover²², and accelerating desertification has been reported during the past half century, caused by the increasing intensity of human exploitation of natural resources^{21–24}. As a result, approximately 0.13 million km² of karst areas previously covered by vegetation and soil were turned into a rocky landscape. To combat this severe form of land degradation and to relieve poverty, more than 130 billion yuan (~19 billion USD) have been invested in mitigation initiatives since the end of the 1990s²⁴. The largest programme implemented, the Grain to Green Project, offers grain, cash and free seedlings as compensation for rural households to re-establish forests, shrub and/or grassland²⁴. The costs of ecological engineering projects as a climate change mitigation measure are however only justified if ecosystem properties can be affected at large scales. If such afforestation projects are to be considered successful, a large-scale improvement in vegetation cover and carbon sequestration is required with a clear relation to the spatial extent of areas selected for conservation projects. If evidence of such large-scale projects can be found, we further expect these increases to be independent from climate trends.

Results

Shifts in satellite time series coincided with conservation project implementation. LAI from GIMMS-3g¹⁰ (1982 to 2015) as well as ABC derived from vegetation optical depth (VOD)¹¹ (1992 to

¹Key Laboratory for Agro-ecological Processes in Subtropical Region, Institute of Subtropical Agriculture, Chinese Academy of Sciences, Changsha, China. ²Department of Geosciences and Natural Resource Management, University of Copenhagen, Copenhagen, Denmark. ³Huanjiang Observation and Research Station for Karst Ecosystem, Chinese Academy of Sciences, Huanjiang, China. ⁴Division of Forest, Nature and Landscape, KU Leuven, Heverlee, Belgium. ⁵Department of Microbiology and Plant Biology, University of Oklahoma, Norman, OK, USA. ⁶Ministry of Education Key Laboratory of Biodiversity and Ecological Engineering, Institute of Biodiversity Science, Shanghai, 200433, China. ⁷Center for Ecosystem Science and Society (Ecos), Department of Biological Sciences, Northern Arizona University, Flagstaff, AZ 86011, USA. ⁸Department of Earth System Science, Tsinghua University, Beijing, 10084, China. ⁹Department of Earth and Environment, Boston University, Boston, MA, USA. Xiaowei Tong and Martin Brandt contributed equally to this work. *e-mail: yymue@isa.ac.cn; kelin@isa.ac.cn

2012) satellite observations were analysed at the regional scale for the Guangxi, Guizhou and Yunnan provinces in southwest China. MODIS LAI²⁵ (hereafter LAI_{modis}) as the state-of-the-art satellite product was included for comparison. To separate climatic drivers from anthropogenic impacts, LAI and ABC were simulated without human influence with the dynamic vegetation model LPJ-GUESS²⁶ (hereafter LAI_{sim} and ABC_{sim}). Breakpoints²⁷ in LAI time series were identified at pixel level and the timing of the observed shifts was analysed. The number of pixels with breakpoints for LAI increased from 1987 to 2009 with most breakpoints detected between 2002 and 2004 (Fig. 1a). The biggest Chinese conservation programme, the Grain to Green Project, was launched in 2000/2001 in

southwest China and most conservation areas were fully implemented in 2002–2004 (Fig. 1b) coinciding with the highest numbers of detected breakpoints. The year 2000 was thus used as a divisor for pre- and post-conservation periods.

The annual ABC¹¹ as well as average growing-season LAI¹⁰ both showed weak positive trends before 2000 ($+0.14 \text{ Mg C ha}^{-1} \text{ y}^{-1}$, $p < 0.01$; $+0.01 \text{ m}^2 \text{ m}^{-2} \text{ y}^{-1}$, $p < 0.05$), which doubled in the post-2000 period ($+0.3 \text{ Mg C ha}^{-1} \text{ y}^{-1}$, $p < 0.01$; $+0.02 \text{ m}^2 \text{ m}^{-2} \text{ y}^{-1}$, $p < 0.05$) (Fig. 1c,e, Fig. 2a). The differences in slopes of both LAI and ABC between the two periods were significant (one-way analysis of variance, $p < 0.01$). After implementation of the conservation projects in 2000, all satellite-based ABC and LAI data sets showed rapid

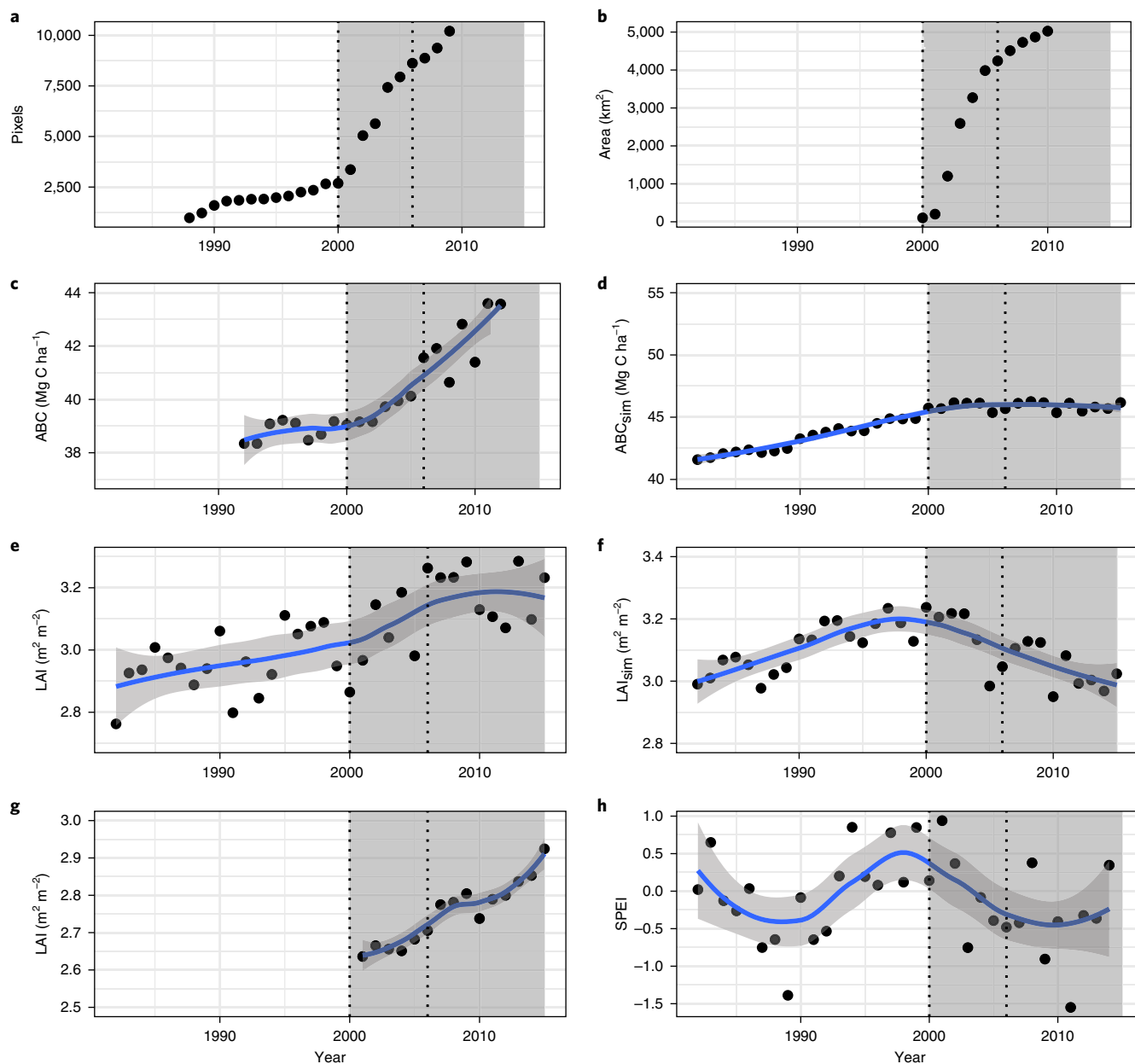


Fig. 1 | Temporal profiles averaged over the three provinces. a, Accumulated breakpoints in LAI satellite time series. **b**, Accumulated areas under conservation. **c**, ABC derived from VOD satellite observations (1992–2012). **d**, Simulated ABC_{sim} from the ecosystem model LPJ-GUESS without anthropogenic influence (1982–2015). **e**, GIMMS-3g LAI (1982–2015). **f**, LPJ-GUESS simulated LAI_{sim} without anthropogenic influence (1982–2015). Pre- and post-conservation periods (before and after 2000) are divided by grey shading. The initial greening phase (2000–2006) is marked with dotted lines. **g**, MODIS LAI_{modis} (2001–2015). Less inter-annual variations and no saturation as compared with GIMMS-3g are explained by the higher sensor and/or production quality and less influence by clouds. **h**, SPEI as drought indicator (1982–2015).

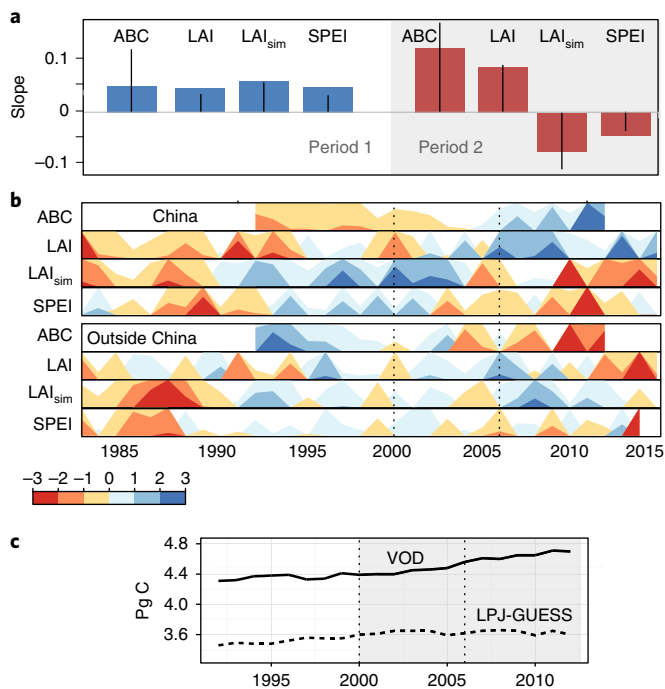


Fig. 2 | Trends, anomalies and carbon stocks. **a**, Median trends (slope of linear regression, no significance mask) of standardized anomalies in observed LAI, ABC, LAI_{sim} and SPEI are shown for two periods (before and after 2000: pre- and post-conservation). Black lines indicate the standard deviation. **b**, Horizon plot of standardized anomalies (collapsed overlapping contours of colours represent the magnitude of the anomaly) in ABC, LAI, LAI_{sim} , SPEI averaged over the three Chinese provinces (Fig. 3a) as well as of the neighbouring countries Myanmar, Laos and Vietnam (average of the areas visible in Fig. 3a). Anomalies show the z-score: $(value - mean) / s.d.$ **c**, Annual carbon stocks estimated from VOD satellite observations and simulated with the ecosystem model LPJ-GUESS. The grey colour in **a** and **c** reflects the post-conservation period.

increases until around 2006 (Fig. 1c,e,g). Whereas GIMMS-3g LAI reached a stable level after this green-up phase, ABC and LAI_{modis} continued to increase. Trends in LAI_{sim} and ABC_{sim} were similar to the observed LAI and ABC in the first period (Fig. 1d,f), but in the second period the temporal development of LAI_{sim} was increasingly diverging from the observed LAI and followed climate conditions characterized by the standardized precipitation–evapotranspiration index (SPEI)²⁸ (Figs. 1h, 2a,b). ABC_{sim} stopped increasing after 2000 (Fig. 1d).

In the spatial domain, ABC and LAI trends were mostly positive over the full period, but negative around urbanized areas (for example, Kunming and Nanning) as well as over agricultural development zones (for example, Baize) (Fig. 3a,b, see Supplementary Figs. 1,2 for LAI_{modis} and LAI_{sim}). The positive trends observed aligned spatially with the Chinese national borders, and LAI and ABC of the neighbouring countries Myanmar, Laos and Vietnam predominantly showed a negative trend, indicating climate- and human-caused forest losses²⁹ (Figs. 2b, 3a,b). LAI trends in several areas were less negative than ABC trends (for example, in Laos) which could be explained by secondary forest regrowth having a similar LAI but a lower ABC than the former primary forest. As LAI_{sim} simulates vegetation changes only from climate forcing data, whereas LAI also includes anthropogenic influence, a decreasing correlation between these two variables indicates an increased human-induced footprint. Indeed, the correlation between simulated LAI_{sim} and observed LAI in China was stronger and positive before 2000 ($r = 0.43$, $p = 0.08$)

but weaker and negative in the later period ($r = -0.32$, $p = 0.2$). Due to long-lasting drought conditions in southwest China in the second period, negative anomalies dominated both LAI_{sim} and SPEI in the later years (Figs. 1f, 2a,b). Negative anomalies were also found in LAI and ABC of China's neighbouring countries, suggesting a stronger impact of climate than was observed in southwest China (Fig. 2b). Overall, comparing observed data and model simulations suggested that the sensitivity of the ecosystem to climate perturbations has been reduced by the intense human management.

Observed increases in carbon stocks. To further quantify the effects of conservation projects, ABC ($Mg\ C\ ha^{-1}$) was converted to carbon stocks (Pg C) for the three provinces. No change was observed in the pre-conservation period with C stocks being stable at ~ 4.3 Pg C (Fig. 2c). C stocks increased after the implementation of conservation areas after 2001 by $\sim 9\%$ to 4.7 Pg C in 2012 ($+0.05$ Pg C y^{-1}) in spite of negative anomalies in SPEI. ABC estimates from the climate-driven ecosystem model LPJ-GUESS did not show a comparable increase in C stocks in the absence of anthropogenic influence.

Trends in LAI and ABC significantly differed with conservation efforts. The effects of conservation projects on LAI and ABC trends were analysed at county level by dividing all counties within the three provinces into four groups according to the total conservation areas of the Grain to Green Project (Fig. 3c, Supplementary Table 1). Trends (linear slopes) for the four groups were determined for two periods, before and after 2000. For the first period, the trends for both LAI and ABC were rather low and of similar magnitude between all groups (Fig. 4a, Supplementary Fig. 3). After implementation of the conservation projects (second period), the trends clearly diverged between the groups. Overall, LAI and ABC showed increasing trends after 2000, however being most pronounced for areas characterized by high conservation efforts. There was no significant difference between the groups for SPEI over the entire period (one-way analysis of variance; $p > 0.9$), but it is notable that negative SPEI anomalies dominated during the past decade, providing less favourable growing conditions for vegetation in the entire region (Fig. 4b). By comparing the pre- and post-conservation project periods, it is clear that the LAI trends reflected the size of the project areas rather than changing climatic conditions (SPEI), which on the other hand controlled the modelled LAI_{sim} (Fig. 4b). Whereas forests were equally distributed among the groups ($\sim 55\%$), the group of highest conservation efforts (group 4) had the highest share of karst areas (70%) and farmlands (28%) (Supplementary Tables 1,2). Contrastingly, the group with the smallest afforestation efforts (group 1) had the lowest share of karsts (34%) and farmlands (18%). Although conservation projects had been implemented all over the three provinces, these differences reflected the high efforts invested into karst area recovery and the conversion of farmland into forests. During the pre-conservation period, group 4 had the lowest LAI (a sign for degraded karst ecosystems), which increased rapidly after 2000 exceeding LAI trends of all other groups (Supplementary Fig. 3). This was also reflected in C stocks, with group 4 showing the largest increase in C stocks (13%), and group 1 only gaining 5%, despite similar C stocks for both groups in 1999 (0.6 Pg C).

Discussion

Our results indicate that afforestation and conservation projects in southwest China can have a remarkable impact on vegetation cover and carbon stocks, which is in line with other research^{2,30–35}. Analysis shows that the total area of conservation projects impacts on leaf area index (LAI) and aboveground biomass carbon (ABC), with strong positive trends in counties of high conservation efforts and corresponding weaker trends in counties of little efforts. The positive trends are shown to demarcate the Chinese national

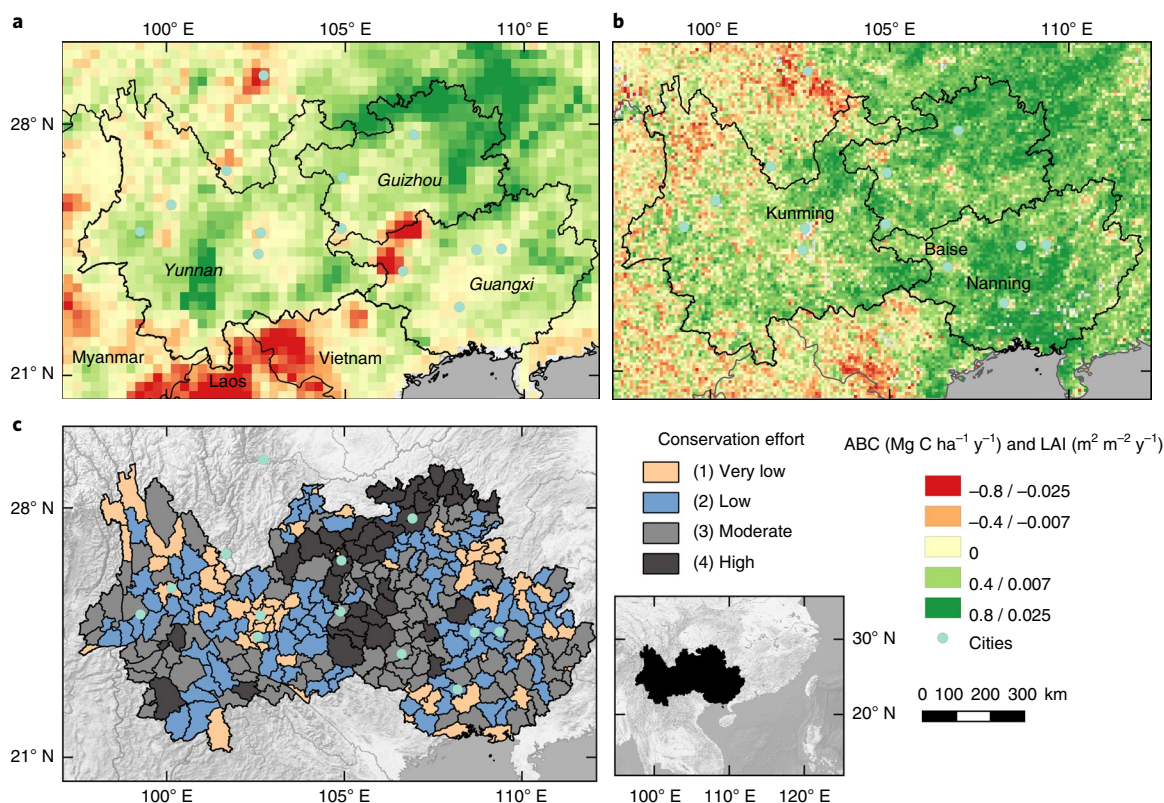


Fig. 3 | The study area includes the provinces Guangxi, Guizhou and Yunnan in southwest China. a, ABC trends (linear slope, $n=21$) from 1992 to 2012. The labels show the three province names and the neighbouring countries Myanmar, Laos and Vietnam. **b**, LAI trends (linear slope, $n=34$) from 1982 to 2015. See Supplementary Figs 1,2 for LAI_{modis} and ecosystem model simulated LAI_{sim} trends. The cities Kunming, Baise and Nanning are labelled. **c**, Division of the counties into four groups according to their total area of conservation projects: (1) less than 50 km² (very low efforts), (2) 50–100 km² (low efforts), (3) 100–200 km² (moderate efforts), and (4) more than 200 km² (high efforts). For more information on the groups, see Supplementary Tables 1,2. No significant difference in SPEI between the four groups was found during the study period (one-way analysis of variance, $p>0.9$, $n=295$).

border; neighbouring countries (Myanmar, Laos and north-eastern Vietnam) clearly show a negative trend in LAI and ABC, following climatic trends but likely also driven by extensive deforestation^{29,35}.

The timing of breakpoints detected in LAI time series agrees well with the implementation and spatial extent of the Grain to Green conservation projects. Ecosystem-model-simulated LAI_{sim} and ABC_{sim} show that the vegetation would have been characterized by a negative trend in the absence of anthropogenic interference after 2001, whereas we observed an increase of 9% ABC, in spite of the occurrence of a widespread drought between 2009 and 2011³⁰. Most of this increase was observed in high conservation areas (group 4), of which a considerable share is located in karst landscapes and farmlands. The greatly increased LAI of these areas is a strong indication that vegetation recovery has occurred during the post-conservation action period. Indeed, official reports based on field assessments document a decrease of rocky desertification by about 10,000 km² between 2005 and 2011³⁶. With a carbon gain rate of +0.05 Pg C y⁻¹, the improved carbon sequestration has turned these regions into a noticeable carbon sink of global impact^{2,11}. For context, an annual carbon loss from deforestation of -0.4 Pg C y⁻¹ for Africa has been reported³⁷, whereas an increase for China of +0.07 Pg C y⁻¹ was found using the same data source¹¹. The annual carbon gain found in the three provinces studied here therefore embodies a considerable part of the total carbon sequestration at the national level.

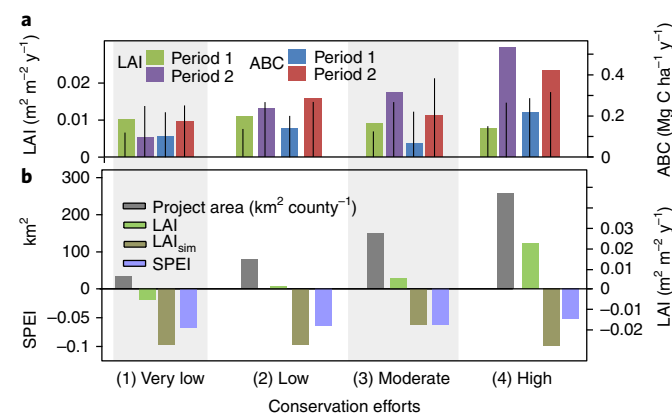


Fig. 4 | Grouped changes in vegetation trends. Magnitude of trends (linear regression slope) of LAI and ABC separated into two periods (before and after 2000: pre- and post-conservation) and grouped according to relative conservation efforts (Supplementary Table 1; Fig. 3c). The same grouping was applied for all sub-figures. Black lines are standard deviations. **b**, Differences between linear trends of two periods (before and after 2000: pre- and post-conservation) are shown for conservation project areas, LAI, LAI_{sim}, and in SPEI. All analyses were conducted at county level ($n=295$).

The use of three independent Earth observation time series all sensing living vegetation supports the direction of our findings. Although LAI derived from GIMMS3g is of lower quality as compared to MODIS LAI, the direction of the trends and the spatial pattern were comparable. Even though the results of each of the conducted analyses leave room for interpretations, taken together, all data sets (based on different satellite platforms, dynamic modelling

and inventory databases) are independent and converge towards the same conclusion: that the conservation projects have remarkably increased the vegetation cover in southwest China.

Other studies highlight the positive indirect effects of anthropogenic activities on woody vegetation growth through altered levels of atmospheric CO₂ and N-deposition^{10,13}. Climatic and atmospheric forcing on vegetation are commonly assessed by dynamic vegetation models, but the ability of models to assess the direct impact of human management is limited. Our simulated LAI_{sim} and ABC_{sim} showed that climatic forcing alone would have led to a considerable decrease in vegetation cover of the region in the latter years (see Supplementary Figs. 4,5 for separated climate and atmospheric forcing). Although this study found a clear pattern at the county level, finer-scaled studies and in situ measurements are necessary to support the surveillance of environmental projects. It has been shown that financial investment and the spatial extent of plantations for environmental restoration or commercial purposes are not linearly linked with an increase in the vegetation abundance, as the effectiveness of implementations varies with topography and management aspects¹⁵. Whereas the satellite-based data applied were able to monitor continuous changes in LAI and ABC, no firm conclusions on changes in species composition and functioning can be drawn and the positive trends may conceal the establishment of monocultures and inappropriate conservation actions. We thus emphasize the need for complementary studies at the local scale using temporal snap-shots of higher resolution satellite imagery in combination with field surveys to also map qualitative aspects of changes in woody vegetation and forests (for example, species composition and biodiversity). It is crucial to accurately assess the efforts and benefits of conservation projects and identify the potential threats to local, regional and national eco-environmental changes from the combined impacts of anthropogenic influence (both overuse and conservation) and climate change.

Methods

Multiple and independent long-term data sets were applied to monitor the impact of conservation projects on leaf area index (LAI) and aboveground biomass carbon (ABC) changes. The high investments in conservation projects as a climate change mitigation measure will only be legitimized if ecosystem properties can be affected on large scales. The analyses were therefore conducted at the county level, which also alleviates scaling issues caused by different data sources. We used statistical data to divide the counties into four groups according to the accumulated areas of conservation projects from the Grain to Green project. Breakpoints were determined for time series of satellite based LAI data.

Growing season average LAI. The growing season spans from April to November in southwest China. Two LAI data sets were used to calculate the growing season average LAI, namely the Boston University reprocessed MODIS Collection 6 LAI (hereafter LAI_{modis}) and the latest GIMMS-3g LAI. LAI quantifies the total area of green elements of the canopy per unit horizontal ground area³⁸. The applied data sets are thus proxies for the total green LAI of all canopy layers, and can be used as a proxy for the green vegetation cover. For this study, all available LAI data that overlap our defined growing season were averaged to provide a proxy for the annual vegetation of a given area.

LAI_{modis}. These data (16-day LAI composite, from 2001–2015) were refined from the standard MODIS Collection 6 LAI product based on the quality flags of MOD15A2H (8-day LAI composite) and MOD13A2 (16-day vegetation index composite). The standard MODIS Collection 6 LAI product was widely used and well validated by the community^{38–40}. The refined LAI data set follows the quality control scheme as described previously⁴⁰ and represents the highest quality MODIS LAI. The refined LAI composite was aggregated to a 5 km × 5 km grid by averaging the available clean LAI values originally at 500-m resolution. According to the definition of LAI, that is, total green leaf area per unit ground, and considering that the coarse grid is often mixed with non-vegetation, each aggregated LAI value is stretched by the percentage of the vegetated area, where the percentage of the vegetated area can be retrieved from the quality flag of MOD15A2H. We re-projected the LAI data set to a 0.05° × 0.05° grid using the nearest-neighbour method. The advantages of this data set include: the bandwidth was specially designed for vegetation monitoring; the signal was well calibrated and stable (that is, no inter-sensor calibration issues); the reflectance was corrected for atmospheric effects; and the quality flags were carefully recorded.

GIMMS-3g LAI. The latest version of GIMMS-3g LAI was generated by training the GIMMS-3gV1 NDVI with LAI_{modis} using an artificial neural network⁴¹. Compared to the previous version of GIMMS-3g LAI, the new version is trained by LAI_{modis} instead of the Beijing Normal University LAI, which was used for previous versions. This data set is available bi-monthly as a 1/12 × 1/12 CMG grid from 1982–2015.

Contrary to LAI, vegetation optical depth (VOD) is sensitive to the water content of all vegetation, including the green and non-green parts (that is, branches and stems of trees)⁴². VOD is thus less prone to saturation and less sensitive to inter-annual variations in climatic conditions. The signal is primarily driven by aboveground biomass which is commonly dominated by woody plants^{13,42}. The long-term VOD data set (1992–2012) is retrieved from satellite passive microwave observations with a spatial resolution of 0.25° × 0.25° (ref. 43).

To quantify changes in aboveground biomass carbon, we used a similar method as proposed previously⁴¹. A benchmark map of carbon density of aboveground living woody vegetation in global tropical areas⁴⁵ was used to establish a relationship with VOD (averaged from 2000 to 2012) using boosted regression trees⁴⁴. The predicted ABC correlates well with the benchmark map ($r=0.88$, slope = 0.74) and the derived coefficients were employed on annual VOD. The result is comparable with that reported previously⁴¹ (annual values $r^2=0.97$) to which we refer for uncertainty analyses. This space for time conversion was applied as no field data based ABC estimates were available for a longer period. Carbon density in Mg C ha⁻¹ was converted to carbon stocks by multiplication with the amount of hectare covered by each pixel. The sum over the study area is the total carbon stock. Finally, both growing season LAI and ABC were averaged at the county level.

Climate data. We applied a standardized precipitation–evapotranspiration index (SPEI) which considers the effect of reference evapotranspiration on drought severity to identify climate change processes^{38,45}. SPEI is based on gridded monthly climate data (temperature, precipitation) from CRU TS 3.24.01⁴⁶. This study focuses on woody vegetation, which does not necessarily react immediately to rainfall fluctuations, and therefore SPEI data integrated over 12 months were chosen as an indicator for vegetation water stress. SPEI data were averaged for each year, resampled to 8-km spatial resolution using a bilinear interpolation, and then aggregated to county level by averaging.

Dynamic vegetation modelling. The vegetation response to natural drivers was simulated with the dynamic vegetation model LPJ-GUESS (ref. 26). LPJ-GUESS represents vegetation with 10 tree plant functional types and 2 grass plant functional types, and within these plant functional types, carbon is represented in four pools: leaves, roots, sapwood and heartwood. LAI and ABC were simulated at 0.5° spatial resolution with a Farquhar-type photosynthesis model⁴⁷ at a daily time step⁴⁸. Simulations with LPJ-GUESS were performed for 1901–2015 applying gridded monthly climate data (temperature, precipitation and cloud cover) from CRU TS 3.24.01⁴⁶, monthly nitrogen deposition⁴⁹, and annual mean atmospheric CO₂ concentration^{50,51} as forcing. The simulation was preceded by a 500-year-long spinup in which the climate forcing was used for 1901–1930, applying the inter-annual variability for this period to capture realistic climatic variations, and 1901 values for atmospheric CO₂ concentration and N deposition were applied. Land use and land use change were not taken into account, to represent the dynamics of the natural vegetation only.

To separate the impact of variations in climate from those of rising atmospheric CO₂ concentration⁵², three additional simulations were performed in which climate drivers (temperature, precipitation and radiation) were kept at the levels of 1962–1981, atmospheric CO₂ was kept at the level of 1981, or both. The impact of climate and CO₂ was determined by subtracting the changes in the latter from those in the former two simulations.

Breakpoint detection. Breaks for additive season and trend (BFAST)²⁷ analysis was applied on LAI at per-pixel level to identify breakpoints in vegetation time series. The timing of the breakpoint was provided with an interval of confidence that can reach approximately ±3 years, which should be kept in mind when interpreting the results. A breakpoint indicates a change in the amplitude and/or direction of vegetation trends and can be induced by climatic or anthropogenic disturbances. It is thus important to inspect the occurrence of breakpoints according to supporting data sources (that is, SPEI, project implementations). It has to be noted that a monotonic and/or insignificant trend can also include a project-induced breakpoint if the magnitude of the trend exhibits a noticeable change. No significance mask was thus applied in this study, all per-pixel breakpoints were considered regardless of their statistical significance. Instead, the plausibility of the timing of the detected point was assessed by comparing the detected years with climate data and timing of conservation project implementations. Due to the longer time period and higher spatial resolution, LAI data were considered better suited for breakpoint detection analysis and VOD breakpoint analyses are shown in the Supplementary Fig. 6. Moreover, biomass does not change equally abruptly, making VOD less suited for breakpoint detection.

Inventory data on the Grain to Green Project. We used statistical data from the Grain to Green Project (GGP) (considered the most ambitious environmental engineering initiative globally^{16,24,53–55}) to relate vegetation trends to conservation projects. The GGP is a nationwide project and was started in 2000 in the Guizhou

province, and continued in the provinces of Guangxi and Yunnan in 2001. During the initial stage (2000–2001), the GGP encompassed 27 counties of the three provinces and was expanded to cover the entire study area in the following years. The primary aim of the GGP in southwest China was to combat ongoing soil erosion and rocky desertification and to promote vegetation cover by converting farmlands located on slopes $> 25^\circ$ into ecological (used for timber production) and economical (orchards or plantations with trees for medical use) forests²⁴. The programme provided resources in the form of grain, cash and free seedlings as incentives for rural households to re-establish forest, shrub and/or grassland on marginal and sloped farmland and shrubland²⁴. The primary selection criterion for areas eligible for restoration projects was the slope of the landscape, but also the soil fertility and the state of erosion or susceptibility to erode^{24,55}. The potential farmer incomes that could be generated were also important factors taken into consideration by the planners of the GGP. Local forestry bureaus managed the selection of trees that may be planted with the financial support of the GGP based on official standards for ecological and economic trees²⁴. Detailed standards for tree planting were imposed taking into consideration the planting density of specific species to avoid soil erosion. As part of the programme design, it was specified that 80% of the trees should be ecological trees and 20% should be economic trees in all administrative units²⁴. This criterion was enforced as economic trees provide fewer ecological services and require more frequent replanting as compared with ecological trees, which may eventually compromise the primary objective of the programme²⁴. Most farmers are inclined to plant economic trees, due to relatively faster and higher revenue from the sale of non-timber products (such as fruits). Additionally, if the fruit production is declining, the trees can be sold as timber²⁴. Contrastingly, ecological trees only generate a limited income through the sale of wood from thinning during the growth phase, and the time before farmers obtain the revenue generated by selling timber is not as fast as compared to the case of economic trees²⁴. Finally, the rules of timber sale are defective as farmers must apply for a logging quota from the forestry bureau and logging permission can be postponed for several years or permission might be given to cut only a fraction of what was originally applied for. In spite of the farmers preferences for growing economic trees, the declared national standard of 80% of the land being reforested with ecological trees is met in most places^{16,24,55}.

The species planted are often not native, and adequate selection of tree species depends to a large extent on the climate and soil conditions, which vary greatly in karst areas of southwest China. The main criterion for species selection is the growth rate of trees, but resistance towards climate variability is also important to maintain a high survival rate. Although the planted species vary between different townships, in reality a limited number of fast-growing species are preferred, effectively creating monocultures^{17,24}. Forests may therefore not be sufficiently diverse to favour a diverse wildlife and the monoculture is also vulnerable to the risks of pests or fires. Yet, low species diversity helps farmers to generate higher economic incomes, which also encourages them to protect the trees in the best possible way²⁴. Previous studies from the area have indicated survival rates of 60–70%^{24,55}, which is relatively high. Fertilizers are used occasionally, but irrigation is not common in the study area. For further details on the GGP, we refer to (ref. ²⁴).

The data for this study were available at county level and included the total area in which conservation actions were applied. As the effectiveness of the implemented conservation varies considerably between counties, this will also be reflected in the afforestation or land cover changes¹⁵. However, the data provide a useful indication on active investments that allows for a detailed analysis of vegetation changes in relation to conservation project efforts. Counties were divided into four groups according to the total area coverage of active conservation projects during the period 2000–2010. The binning was determined based on a requirement of a balanced number and spatial distribution of counties included in each group. Group 1 (very-low efforts) includes less than 50 km² of conservation areas for each county, group 2 50–100 km² (low efforts), group 3 100–200 km² (moderate efforts), and group 4 more than 200 km² (high efforts). To test for significant differences in SPEI, LAI_{min} and LAI between the four groups, we applied a one-way analysis of variance.

Data availability. LAI derived from GIMMS-3g v. 1 and MODIS are available from Boston University (<http://cliveg.bu.edu/modismisr/lai3g-fpar3g.html>), VOD data were provided by Y. Liu (available at <http://www.wenfo.org/wald/global-biomass/>). SPEI data can be obtained at <http://spei.csic.es/database.html>. Statistical data on the Grain to Green project were provided by the Forestry Bureau of the Yunnan, Guizhou and Guangxi Provinces. Results from the dynamic vegetation model are available from the corresponding authors upon request.

Received: 16 June 2017; Accepted: 27 November 2017;
Published online: 8 January 2018

References

- Martinez-Ramos, M. et al. Anthropogenic disturbances jeopardize biodiversity conservation within tropical rainforest reserves. *Proc. Natl Acad. Sci. USA* **113**, 5323–5328 (2016).
- Fang, J. et al. Forest biomass carbon sinks in East Asia, with special reference to the relative contributions of forest expansion and forest growth. *Glob. Change Biol.* **20**, 2019–2030 (2014).
- Zhou, L. et al. Widespread decline of Congo rainforest greenness in the past decade. *Nature* **509**, 86–90 (2014).
- Piao, S. et al. Detection and attribution of vegetation greening trend in China over the last 30 years. *Glob. Change Biol.* **21**, 1601–1609 (2015).
- Schwalm, C. R. et al. Global patterns of drought recovery. *Nature* **548**, 202–205 (2017).
- Doughty, C. E. et al. Drought impact on forest carbon dynamics and fluxes in Amazonia. *Nature* **519**, 78–82 (2015).
- Kharin, V. V., Zwiers, F. W., Zhang, X. & Hegerl, G. C. Changes in temperature and precipitation extremes in the IPCC ensemble of global coupled model simulations. *J. Clim.* **20**, 1419–1444 (2007).
- Seddon, A. W. R., Macias-Fauria, M., Long, P. R., Benz, D. & Willis, K. J. Sensitivity of global terrestrial ecosystems to climate variability. *Nature* **531**, 229–232 (2016).
- Lloret, F., Escudero, A., Iriondo, J. M., Martínez-Vilalta, J. & Valladares, F. Extreme climatic events and vegetation: the role of stabilizing processes. *Glob. Change Biol.* **18**, 797–805 (2012).
- Zhu, Z. et al. Greening of the Earth and its drivers. *Nat. Clim. Change* **6**, 791–795 (2016).
- Liu, Y. Y. et al. Recent reversal in loss of global terrestrial biomass. *Nat. Clim. Change* **5**, 470–474 (2015).
- Fensholt, R. et al. Greenness in semi-arid areas across the globe 1981–2007 — an Earth Observing Satellite based analysis of trends and drivers. *Remote Sens. Environ.* **121**, 144–158 (2012).
- Brandt, M. et al. Human population growth offsets climate-driven increase in woody vegetation in sub-Saharan Africa. *Nat. Ecol. Evol.* **1**, 0081 (2017).
- Hansen, M. C. et al. High-resolution global maps of 21st-century forest cover change. *Science* **342**, 850–853 (2013).
- Tong, X. et al. Quantifying the effectiveness of ecological restoration projects on long-term vegetation dynamics in the karst regions of southwest China. *Int. J. Appl. Earth Obs. Geoinf.* **54**, 105–113 (2017).
- Ouyang, Z. Y. et al. Improvements in ecosystem services from investments in natural capital. *Science* **352**, 1455–1459 (2016).
- Hua, F. et al. Opportunities for biodiversity gains under the world's largest reforestation programme. *Nat. Commun.* **7**, 12717 (2016).
- Moore, J. C. et al. Will China be the first to initiate climate engineering? *Earth's Future* **4**, 588–595 (2016).
- Xu, W. et al. Strengthening protected areas for biodiversity and ecosystem services in China. *Proc. Natl Acad. Sci. USA* **114**, 1601–1606 (2017).
- Jiang, Z. C., Lian, Y. Q. & Qin, X. Q. Rocky desertification in Southwest China: Impacts, causes, and restoration. *Earth Sci. Rev.* **321**, 1–12 (2014).
- Sweeting M. M. *Karst in China: Its Geomorphology and Environment* (Springer, Berlin, New York, 2012).
- Miao, Z. L. Xu Xiak'e's contributions to karst study in Southwestern China. *Geogr. Res.* **5**, 18–24 (1986).
- Zhang, C., Qi, X., Wang, K., Zhang, M. & Yue, Y. The application of geospatial techniques in monitoring karst vegetation recovery in southwest China: a review. *Progr. Phys. Geogr.* **41**, 450–477 (2017).
- Delang, C. O. & Yuan, Z. *China's Grain for Green Program* (Springer, Heidelberg, 2015).
- Yan, K. et al. Evaluation of MODIS LAI/FPAR Product Collection 6. Part 1: consistency and improvements. *Remote Sens.* **8**, 359–16 (2016).
- Smith, B. et al. Implications of incorporating N cycling and N limitations on primary production in an individual-based dynamic vegetation model. *Biogeosciences* **11**, 2027–2054 (2014).
- de Jong, R., Verbesselt, J., Zeileis, A. & Schaepman, M. E. Shifts in global vegetation activity trends. *Remote Sens.* **5**, 1117–1133 (2013).
- Beguieria, S., Vicente-Serrano, S. M., Reig, F. & Latorre, B. Standardized precipitation evapotranspiration index (SPEI) revisited: parameter fitting, evapotranspiration models, tools, datasets and drought monitoring. *Int. J. Climatol.* **34**, 3001–3023 (2014).
- Grogan, K., Pflugmacher, D., Hostert, P., Kennedy, R. & Fensholt, R. Cross-border forest disturbance and the role of natural rubber in mainland Southeast Asia using annual Landsat time series. *Remote Sens. Environ.* **169**, 438–453 (2015).
- Peng, S. et al. Recent change of vegetation growth trend in China. *Environ. Res. Lett.* **6**, 044027 (2011).
- Zhang, Y. et al. Multiple afforestation programs accelerate the greenness in the 'Three North' region of China from 1982 to 2013. *Ecol. Indic.* **61**, 404–412 (2016).
- Xiao, J. Satellite evidence for significant biophysical consequences of the 'Grain for Green' Program on the Loess Plateau in China. *J. Geophys. Res. Biogeosci.* **119**, 2014JG002820 (2014).
- Li, S. et al. Vegetation changes in recent large-scale ecological restoration projects and subsequent impact on water resources in China's Loess Plateau. *Sci. Total Environ.* **569–570**, 1032–1039 (2016).

34. Cai, H., Yang, X., Wang, K. & Xiao, L. Is forest restoration in the Southwest China Karst promoted mainly by climate change or human-induced factors? *Remote Sens.* **6**, 9895–9910 (2014).
35. Meyfroidt, P. & Lambin, E. F. Forest transition in Vietnam and its environmental impacts. *Glob. Change Biol.* **14**, 1319–1336 (2008).
36. *Bulletin of China's Rocky Desertification* (State Forestry Administration of China, 2012); <http://www.forestry.gov.cn/portal/zsxh/s/3445/content-548741.html>.
37. Houghton, R. A. & Nassikas, A. A. Global and regional fluxes of carbon from land use and land cover change 1850–2015. *Glob. Biogeochem. Cycles* **31**, 2016GB005546 (2017).
38. Yan, K. et al. Evaluation of MODIS LAI/FPAR Product Collection 6. Part 2: validation and intercomparison. *Remote Sens.* **8**, 460–426 (2016).
39. Myneni, R. B. et al. Global products of vegetation leaf area and fraction absorbed PAR from year one of MODIS data. *Remote Sens. Environ.* **83**, 214–231 (2002).
40. Samanta, A. et al. Comment on 'drought-induced reduction in global terrestrial net primary production from 2000 through 2009'. *Science* **333**, 1093–1093 (2011).
41. Zhu, Z. et al. Global data sets of vegetation leaf area index (LAI)3g and fraction of photosynthetically active radiation (FPAR)3g derived from global inventory modeling and mapping studies (GIMMS) normalized difference vegetation index (NDVI3g) for the period 1981 to 2011. *Remote Sens.* **5**, 927–948 (2013).
42. Tian, F., Brandt, M., Liu, Y. Y., Rasmussen, K. & Fensholt, R. Mapping gains and losses in woody vegetation across global tropical drylands. *Glob. Change Biol.* **4**, 1748–1760 (2017).
43. Baccini, A. et al. Estimated carbon dioxide emissions from tropical deforestation improved by carbon-density maps. *Nat. Clim. Change* **2**, 182–185 (2012).
44. Breiman, L. *Arcting the Edge* (Statistics Department, Univ. California, Berkeley, 1997).
45. Vicente-Serrano, S. M., Beguería, S., López-Moreno, J. I., Angulo, M. & El Kenawy, A. A New global 0.5° gridded dataset (1901–2006) of a multiscale drought index: comparison with current drought index datasets based on the Palmer drought severity index. *J. Hydrometeor.* **11**, 1033–1043 (2010).
46. Harris, I., Jones, P. D., Osborn, T. J. & Lister, D. H. Updated high-resolution grids of monthly climatic observations – the CRU TS3.10 dataset. *Int. J. Climatol.* **34**, 623–642 (2014).
47. Farquhar, G. D., Von Caemmerer, S. & Berry, J. A. A biochemical model of photosynthetic CO₂ assimilation in leaves of C₃ species. *Planta* **149**, 8–90 (1980).
48. Haxeltine, A. & Prentice, I. C. A general model for the light-use efficiency of primary production. *Func. Ecol.* **10**, 551–561 (1996).
49. Lamarque, J.-F. et al. Multi-model mean nitrogen and sulfur deposition from the Atmospheric Chemistry and Climate Model Intercomparison Project (ACCMIP): evaluation of historical and projected future changes. *Atmos. Chem. Phys.* **13**, 7997–8018 (2013).
50. Etheridge, D. M. et al. Natural and anthropogenic changes in atmospheric CO₂ over the last 1000 years from air in Antarctic ice and firn. *J. Geophys. Res. Atmos.* **101**, 4115–4128 (1996).
51. Keeling, C. D., Whorf, T. P., Wahlen, M. & van der Plicht, J. Interannual extremes in the rate of rise of atmospheric carbon dioxide since 1980. *Nature* **375**, 666–670 (1995).
52. Keenan, T. F. et al. Recent pause in the growth rate of atmospheric CO₂ due to enhanced terrestrial carbon uptake. *Nat. Commun.* **7**, 13428 (2016).
53. Liu, J., Li, S., Ouyang, Z., Tam, C. & Chen, X. Ecological and socioeconomic effects of China's policies for ecosystem services. *Proc. Natl Acad. Sci. USA* **105**, 9477–9482 (2008).
54. Xu, Z., Bennett, M. T., Tao, R. & Xu, J. China's sloping land conversion program four years on: current situation and pending issues. *Int. Forest. Rev.* **6**, 317–326 (2004).
55. Trac, C. J., Harrell, S., Hinckley, T. M. & Henck, A. C. Reforestation programs in southwest China: reported success, observed failure, and the reasons why. *J. Mt. Sci.* **4**, 275–292 (2007).

Acknowledgements

The study was funded by the National Key Research and Development Program of China (no. 2016YFC0502400) and National Natural Science Foundation of China (no. 41471445, 41371418) and Science and Technology Service Network Initiative of Chinese Academy of Sciences (no. KFJ-STZ-DTP-036). M.B. received funding from the European Union's Horizon 2020 Research and Innovation programme under Marie Skłodowska-Curie grant agreement no. 656564. R.F. acknowledges funding from the Danish Council for Independent Research (DFR) grant ID: DFF-6111-00258.

Author contributions

X.T., M.B., R.F., S.H., Y.Y., W.K. and K.W. designed the study. X.T., S.H. (BFAST), W.K. and G.S. (LPJ) conducted the analyses with support from F.T., Y.Y., M.B. and R.F. MODIS and LAI data were prepared by R.M. and C.C.; M.B. and X.T. drafted the manuscript, which was edited by R.F., S.H., W.K., Y.Y., G.S., F.T., Z.S., X.X., C.C., H.C. and Y.L.

Competing interests

The authors declare no competing financial interests.

Additional information

Supplementary information is available for this paper at <https://doi.org/10.1038/s41893-017-0004-x>.

Reprints and permissions information is available at www.nature.com/reprints.

Correspondence and requests for materials should be addressed to Y.Y. or K.W.

Publisher's note: Springer Nature remains neutral with regard to jurisdictional claims in published maps and institutional affiliations.